

Kelly, G., A. McNally, J.-N. Thépaut & M. Szyndel, 2004. Observing System Experiments of all main data types in the ECMWF operational system. In Proc. of the Third WMO Workshop on the Impact of Various Observing Systems on NWP, Alpbach, Austria, 9–12 March 2004.

McNally, A.P., P.D. Watts, J.A. Smith, R. Engelen, G. Kelly, J.-N. Thépaut & M. Matricardi, 2004: The assimilation of AIRS

radiance data at ECMW. In *Workshop on Assimilation of High Spectral Resolution Sounders in NWP*, 28 June–1 July 2004, Shinfield Park, Reading 73–88.

Thépaut, J.-N. & G.A. Kelly, 2007. Relative contributions from various terrestrial observing systems in the ECMWF NWP system. *Final Report EUCOS*, 23 June 2007 (available from EUCOS Secretariat).

Impact of airborne Doppler lidar observations on ECMWF forecasts

MARTIN WEISSMANN, CARLA CARDINALI

THE WIND field over oceans is still poorly observed. Single-level wind measurements are provided at the surface by buoys, ships and satellite scatterometers, while aircraft observe wind mainly at the cruise level along the air traffic corridors. Wind profiles are only provided by a small number of radiosondes launched from ships. Satellite cloud-drift winds are numerous, but they have fairly large errors due to inaccurate height assignment. In such a framework, Doppler wind lidar offers a great opportunity to measure the wind field either globally with a polar-orbiting satellite or regionally when mounted on aircraft.

During the Atlantic THORPEX Regional Campaign (A-TReC) in autumn 2003, the airborne Doppler lidar of the Deutsches Zentrum für Luft- und Raumfahrt (DLR) was used to observe wind profiles over the Atlantic Ocean. In eight flights, the system measured a total of 1,600 profiles that were used experimentally in the global assimilation system at ECMWF. These lidar observations had a significant impact on the analyses as well as on forecasts due to their high accuracy and spatial resolution. On average, the measurements reduced the forecast error of geopotential height for days 2–4 over Europe by 3%. Furthermore, forecast errors of wind, temperature and humidity fields over Europe were reduced. This is a promising result, considering that observations have been gathered from only 28.5 flight hours in a two-week period. Dropsondes released in the same area where the Doppler lidar was operating showed good agreement in terms of measured winds, but smaller analysis impact and less reduction of the forecast error. A detailed assessment of the experiments can be found in *Weissmann & Cardinali (2007)*.

AFFILIATIONS

Martin Weissmann: Institut für Physik der Atmosphäre, DLR Oberpfaffenhofen, Postfach 1116, 82230 Weßling, Germany
Carla Cardinali: ECMWF, Shinfield Park, Reading, RG12 9AX, UK

The airborne Doppler lidar system

The principle of Doppler lidar is in many ways similar to that of Doppler radar except that a lidar emits pulses of laser light instead of radio waves. The airborne DLR Doppler lidar system measures wind profiles beneath the aircraft using the velocity-azimuth display (VAD) technique. The instrument performs a conical step-and-stare scan around the vertical axis at 20° off nadir. At 24 different azimuth angles, the lidar emits 500 or 1,000 laser pulses at a wavelength of ~2.02 µm and measures the backscatter signal from atmospheric aerosols. The Doppler shift of the backscatter signal is proportional to the velocity component in the pointing direction; this is the line-of-sight (LOS) velocity. Wind profiles are usually derived from 24 or 96 LOS profiles. The vertical resolution of the profiles is 100 m.

Combined with the movement of the aircraft the conical scanning leads to a cycloid scan pattern beneath the aircraft and the derived winds are averaged along this scan. This horizontal averaging is the main advantage of airborne Doppler lidar observations compared to in-situ observations as it makes the data more representative of the wind in a model grid box. The horizontal width of the scan pattern is up to ~7 km. During A-TReC, the horizontal length of one scanner revolution was usually ~10 km.

Lidar observations during A-TReC

The airborne Doppler Lidar operated from the DLR Falcon aircraft during eight flights between 14 and 28 November 2003 (Figure 1). Four of these flights were part of targeted campaigns. These observations were guided by sensitive area calculations carried out at ECMWF and other meteorological services using singular vectors and ensemble methods. The other four flights were designed for other objectives, but were also used for the impact study. Several people from DLR made a vital contribution to the collection of data: Andreas Dörnbrack organized the field campaign, and Stephan Rahm and Rudolf Simmet were responsible for the unique lidar measurements. Milan Dragosavac (ECMWF) converted the lidar data to BUFR format so that it could be assimilated in the ECMWF system.

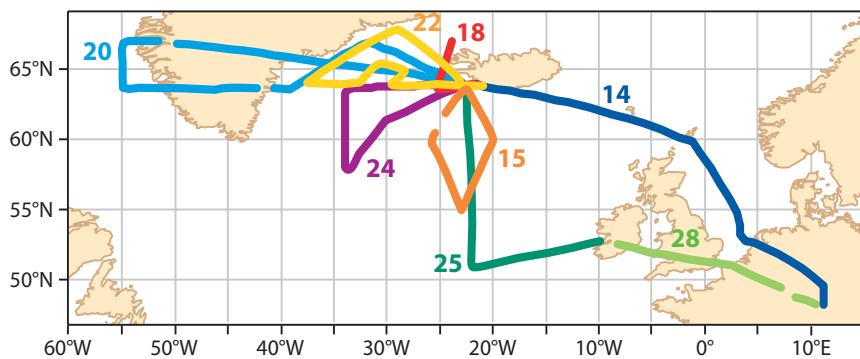


Figure 1 Flight tracks of all flights during A-TReC. Numbers indicate the date of the flights in November 2003.

The data was processed with a horizontal resolution of ~10 km (one scanner revolution) and in parallel also with ~40 km (four scanner revolutions) to increase the measurement coverage and to reduce representativeness errors. The 10 km dataset consists of ~1,600 vertical profiles (~40,000 observations) and the 40-km dataset contains ~400 profiles (~15,000 observations). The vertical cross-section along the aircraft flight track accounts for 36% and 54% data coverage for the 10 km and 40 km resolution, respectively. Missing values in the data are either due to clear air with low aerosol content or to optically thick clouds that cannot be penetrated by the lidar. The number of measurements during the two weeks was fairly evenly distributed between the ground and 10.5 km altitude, the maximum aircraft flight level.

The standard deviation of the instrumental error was determined to be in the range of 0.75–1.0 ms⁻¹ through an intercomparison of collocated dropsonde and lidar measurements. The total error for the assimilation of such measurements (instrumental and representativeness errors) was estimated to be 1.0–1.5 ms⁻¹ for all model levels. This is smaller than the errors of all current routine observations: at ECMWF the error standard deviation of 1.8–3.0 ms⁻¹ is assigned to radiosonde and dropsonde wind observations, 2.5–3.4 ms⁻¹ to aircraft measurements, and 2.0–5.7 ms⁻¹ to satellite cloud-drift winds.

A detailed description of the intercomparison of lidar and dropsonde measurements can be found in Weissmann *et al.* (2005) or online at www.pa.op.dlr.de/natrec/. These sources of information also provide a comprehensive overview of the lidar measurements during A-TReC and a full explanation of the airborne Doppler lidar system.

Experimental setup

Experiments were performed using the ECMWF Model at T511L60 resolution with a 12-hour window 4D-Var. The lidar observations were assimilated as aircraft in-situ observations, but with reduced observation errors. The assimilation of aircraft observations includes a first-guess check eliminating values whose background departures exceed five times that expected. The meas-

urements are thinned to the model resolution to avoid potential imbalances. After the first-guess check, a variational quality control (VarQC) is performed in the minimization procedure to decrease the weight of remaining doubtful observations.

Six experiments were conducted as outlined in Table 1. The control run (*Control*) used all routine observations. All other experiments assimilated either lidar or dropsonde observations in addition to the routine observations. The exper-

iment *1Rev* assimilated lidar wind profiles at a horizontal resolution of ~10 km (the standard resolution of the lidar measurements). Two experiments (*Median* and *4Rev*) were performed with lidar observations horizontally averaged to ~40 km. The purpose of *Median* and *4Rev* was to investigate how much the representativeness of the measurements increases by averaging the data horizontally to the model resolution.

In all these experiments an error standard deviation of 1 ms⁻¹ was assigned to the lidar data at all vertical levels. This error was derived by an intercomparison of collocated lidar and dropsonde measurements, which showed that there is no significant correlation of accuracy and height (Weissmann *et al.*, 2005). The derived error assumes a continuous lidar measurement through a grid box, whereas in reality there were gaps in the measurements due to low aerosol concentrations or clouds. Therefore, the experiment *4RStd* was performed using the same pre-processed lidar data as *4Rev*, but with an error of 1.5 ms⁻¹ to take gaps in the observations into account.

Experiment	Period	Measurements and characteristics of experiments
Control	17 October–15 December	All measurements of the operational analysis without special A-TReC data (dropsondes, AMDAR, etc.)
1Rev	14–30 November	Lidar wind from one scan revolution, horizontal resolution ~10 km, lidar STD = 1 ms ⁻¹
Median	14–30 November	Median of lidar winds from one scan revolution, horizontal resolution ~40 km, lidar STD = 1 ms ⁻¹
4Rev	14–30 November	Lidar wind from four scan revolutions, horizontal resolution ~40 km, lidar STD = 1 ms ⁻¹
4RStd	14–30 November	Same lidar measurements as in 4Rev, but higher measurement error with lidar STD = 1.5 ms ⁻¹
Drops	14–30 November	Dropsonde wind and temperature measurements, 97 sondes, dropsonde STD = 2–3 ms ⁻¹

Table 1 Overview of experiments. The STD refers to the assigned standard deviation of the wind error.

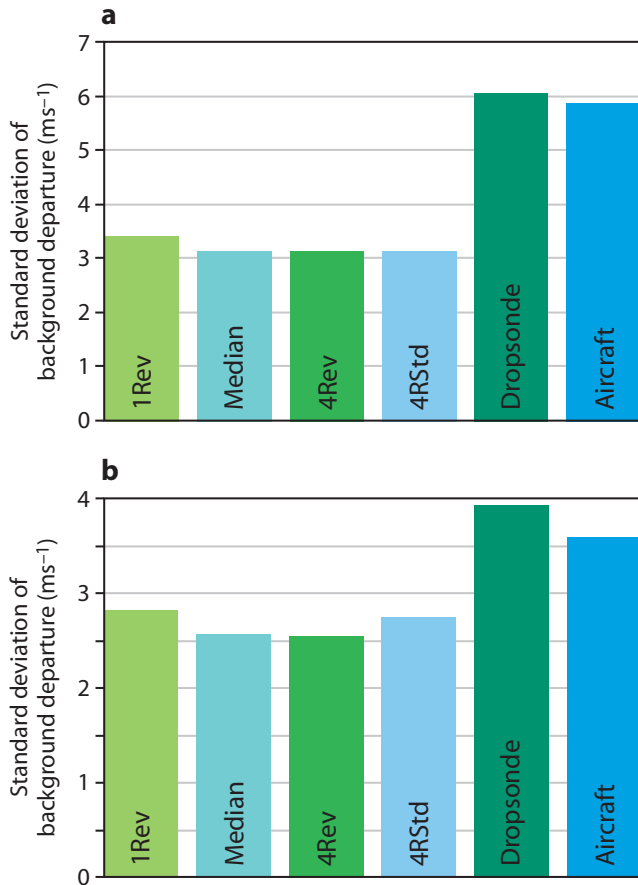


Figure 2 Standard deviations of (a) background departures of all measurements and (b) background departures of observations that are not discarded by the first-guess check or VarQC. The statistics for aircraft and dropsonde measurements are shown for 4RStd and for the area 50°N–70°N, 40°W–15°W (main lidar operating area).

The experiment *Drops* assimilated 97 dropsondes (wind and temperature profiles) released on ten flights in the same period. About half of the dropsondes coincided with lidar measurements. The flight time for the dropsonde observations was similar to that for the lidar measurements. This makes the lidar and dropsonde experiments comparable in terms of observational costs. All experiments were run from 14 to 30 November 2003.

Analysis impact

Assimilation statistics

To investigate the performance of Doppler lidar measurements in the analysis, their background departures from the eight analyses with lidar measurements are sampled and compared to the background departures of aircraft and dropsonde measurements in the same area and at the same time (Figure 2). The variability of lidar background departures is smaller than that of aircraft and dropsonde measurements in the same region. This confirms that lidar winds are more representative of the wind for each model grid box.

The statistics show an improved representativeness of the observations by averaging the measurements

towards the model resolution: on average, the standard deviation of the lidar background departures is about 0.3 ms⁻¹ smaller in the experiments with averaged data (*Median*, *4Rev*) than in the experiment with a 10 km resolution (*1Rev*). There are no significant differences between *Median* and *4Rev*, and at this stage it is not possible to determine which averaging method is best.

Influence of observations

The influence of observations in the analysis can be calculated during the minimization by finding the diagonal elements of the influence matrix (*Cardinali et al.*, 2004). When the influence is 0, the analysis at the observation location is affected only by the background value (or pseudo-observation), while 1 means that only the observation counts in the final estimation at that location.

Figure 3 shows the vertically averaged influence of dropsonde and lidar observations on 22 November 2003. The influence of both observation types is high because the measurements were taken in a data-sparse sensitive region. The mean influence of dropsonde and lidar wind observations is 0.45 and 0.63, respectively. In comparison, the mean observation influence of operational radiosondes in the northern hemisphere extratropics is ~0.3, and the mean influence of aircraft measurements and cloud-drift winds is 0.15 (*Cardinali et al.*, 2004).

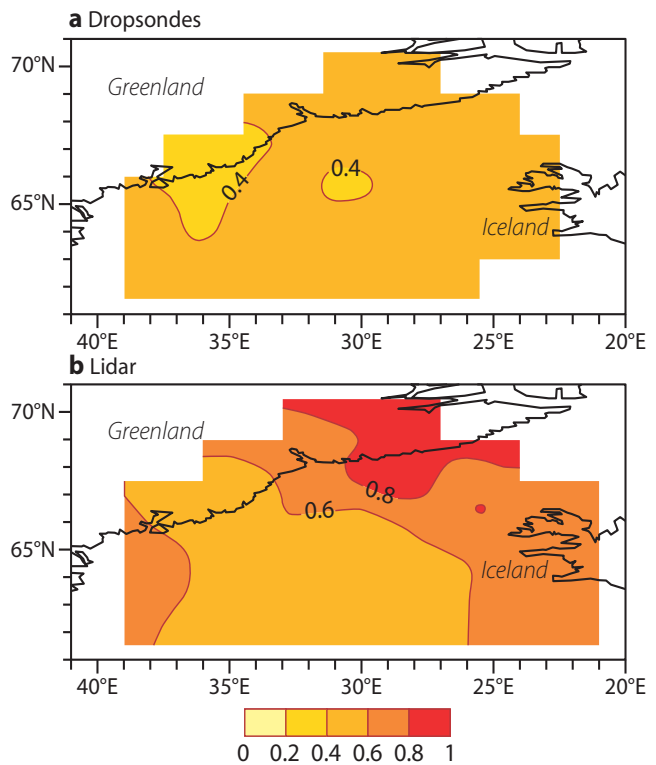


Figure 3 Vertically averaged observation influence on 22 November 2003 for (a) dropsonde wind measurements from *Drops* and (b) lidar wind measurements from 4RStd. Numbers close to one indicate that the analysis is primarily based on the measurements, whereas numbers close to zero mean that the analysis is close to the background field.

The mean lidar observation influence is 40% larger than the mean influence of dropsonde wind measurements. Additionally, the number of lidar observations is about twice as large as the number of dropsonde observations because the horizontal resolution is higher for the lidar. This leads to an information content that is nearly three times higher for the lidar than for the dropsonde observations.

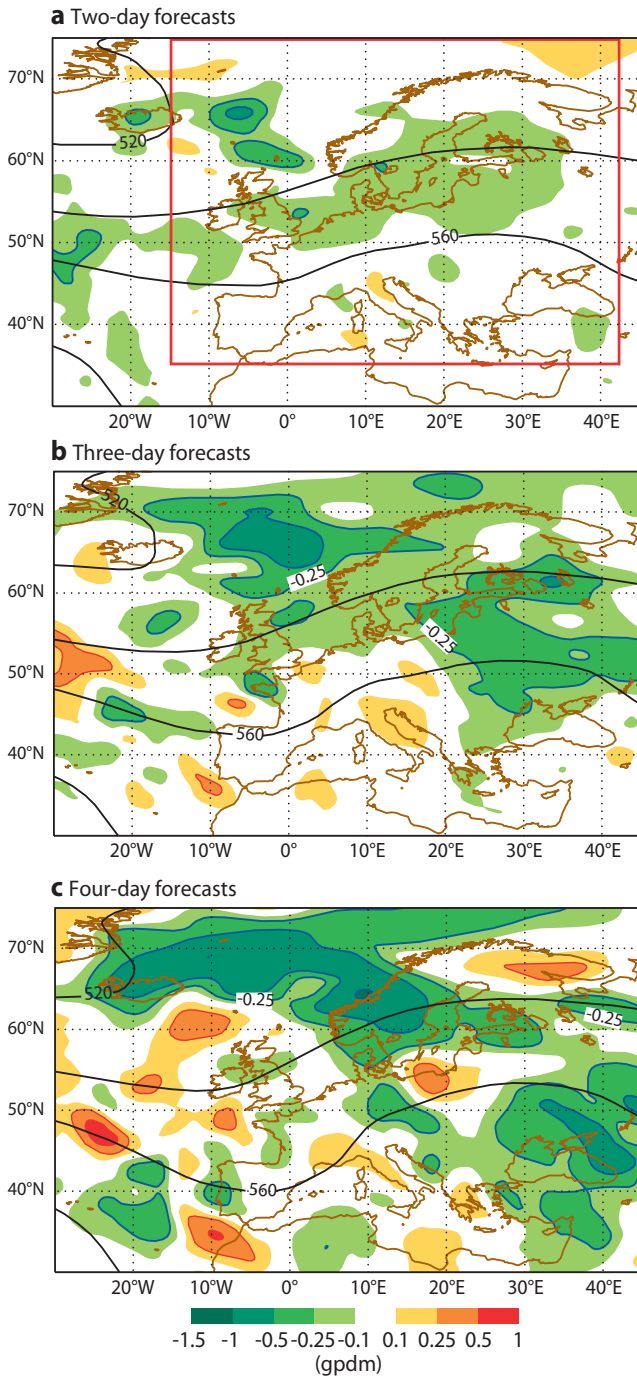


Figure 4 Difference of the root mean square errors of the geopotential height at 500 hPa (gpdm) between *4RStd* and *Control* for (a) two-day forecasts, (b) three-day forecasts and (c) four-day forecasts between 15 and 28 November 2003 (28 forecasts). Negative values indicate a reduction of the forecast error. The box in (a) shows the verification area “Europe” used in this study.

Forecast impact

Figure 4 shows the difference in terms of root mean square forecast error of 500 hPa geopotential height (*Z*) between *4RStd* and *Control* for the period 15–28 November 2003. There is a clear reduction of the two-day forecast error over the Atlantic Ocean and Northern Europe. At day 3 the reduction increases and propagates further to the east. The four-day forecast error also decreases with the lidar measurements and the main reduction of forecast errors is located over the Middle East, and Northern and Eastern Europe. The improvement of one-day forecasts (not shown) was fairly small and mostly restricted to the Atlantic Ocean.

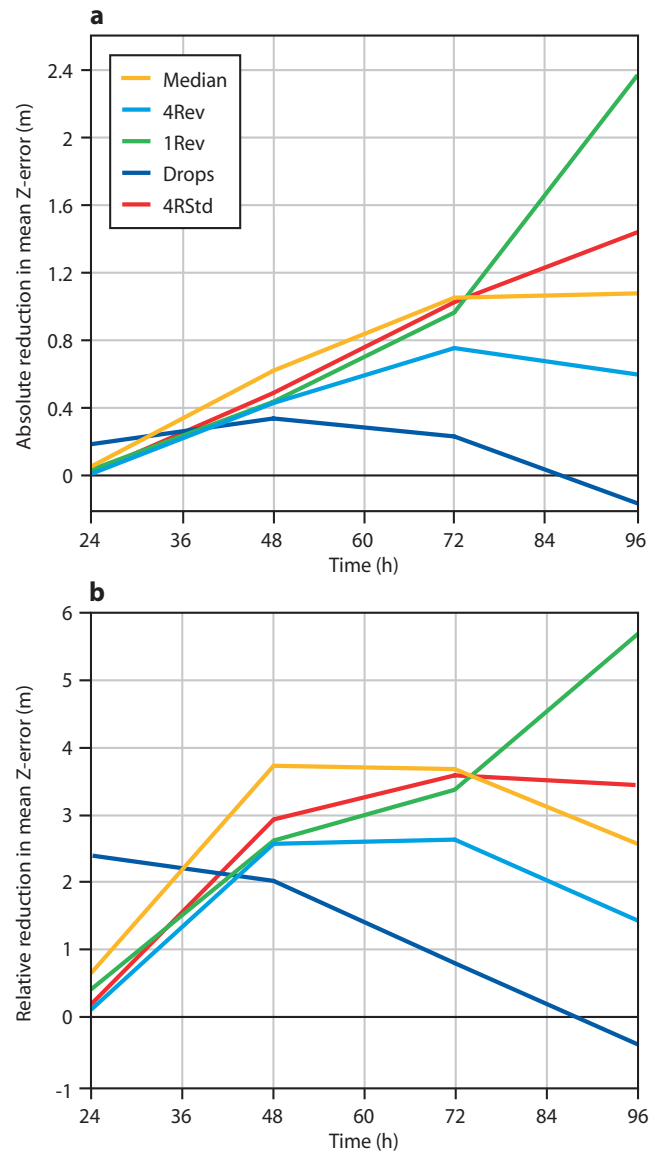


Figure 5 Mean reduction of errors of the geopotential height at 500 hPa over Europe in different experiments compared to *Control*: (a) absolute reduction in metres and (b) relative reduction as a percentage of the mean error of *Control*. Positive values correspond to a smaller error in the experiment than in *Control*. The forecast error is averaged over all forecasts between 12 UTC on 14 November and 12 UTC on 28 November 2003 (29 forecasts). The verification area (“Europe”) is shown in Figure 4(a).

In order to quantify the impact, the forecast error is averaged for Z, wind and humidity for all levels over a box 35°N–75°N and 15°W–42.5°E (see Figure 4) and over 29 forecasts in the period of the lidar deployment. All experiments with lidar data show a Z-error reduction of the forecasts for days 1–4 over Europe compared to *Control* (Figure 5). The experiments *Median* and *4Rev* do not have smaller forecast errors than *1Rev*, although they show better departure statistics. At this stage it is not possible to explain why *1Rev* shows the largest improvement of all experiments at day 4.

The Z-error reduction increases with forecast time up to ~2 m for the four-day forecast. The increase is roughly proportional to the increase of forecast errors, and consequently the relative reduction of Z-errors remains fairly steady around 3% for the forecasts for days 2–4. On average about 60% of the 29 forecasts improved. The spread between the different lidar experiments increases with time indicating the uncertainty due to the small sample of 29 forecasts. The impact after five days is not significant. A larger data sample would be necessary to investigate the long-term impact.

In many experiments the reduction of the Z-error in the forecast is largest in the upper troposphere (Figure 6). The maximum reduction of all experiments is 3 m at 300 hPa for the four-day forecast. The impact extended vertically up to 100 hPa by the background covariance matrix, which is well above the highest lidar measurements at ~250 hPa. The maximum relative reduction of the Z-error for days 2–4 was up to 6%.

The experiment *Drops* also shows a reduction of the Z-error over Europe, mainly at days 1 and 2. At day 3 the reduction is fairly low and at day 4 some degradation above 700 hPa is observed. In general, experiments with lidar data show a larger and more sustained reduction of the forecast error than *Drops*, which is consistent with their larger impact on the analysis.

Wind errors decrease in a similar way as the Z-errors (Figure 7(a)). The relative reduction of wind errors in the troposphere is in the range 0.4–3.3%, which is slightly smaller than the reduction of Z-errors. Furthermore, the lidar wind measurements improve the accuracy of the humidity forecasts (Figure 7(b)) as an improved forecast of the wind and Z-field also leads to a more accurate forecast of humidity structures. The magnitude of the reduction is in the range 0–2%. The reduction of forecast errors of humidity for days 3–4 show maxima at 700 and 850 hPa that are presumably related to an improved prediction of frontal systems.

To sum up

Despite recent advances in the use of satellite observations, there is a drastic shortage of wind measurements over the oceans. This is a major deficiency in NWP as wind information has been shown to be of particular importance for representing dynamical fields in the forecast (*Cress & Wergen, 2001*). Thus, Doppler lidar measurements with their high accuracy and high resolution are a promising source of information to reduce errors in NWP models.

For the first time, airborne Doppler wind lidar observations were assimilated in a global model in the framework of A-TReC. The experiments confirmed that airborne lidar observations are more representative of the wind in a model grid box. Thus the resulting assigned observation error variability (instrumental and representativeness error) is about half that of most conventional observations. The mean lidar observation influence (i.e. the impact on the analysis) is found to be 40% higher than the influence of dropsonde wind measurements. Furthermore, it is shown that lidar wind observations have a significant impact on analysis and forecast errors.

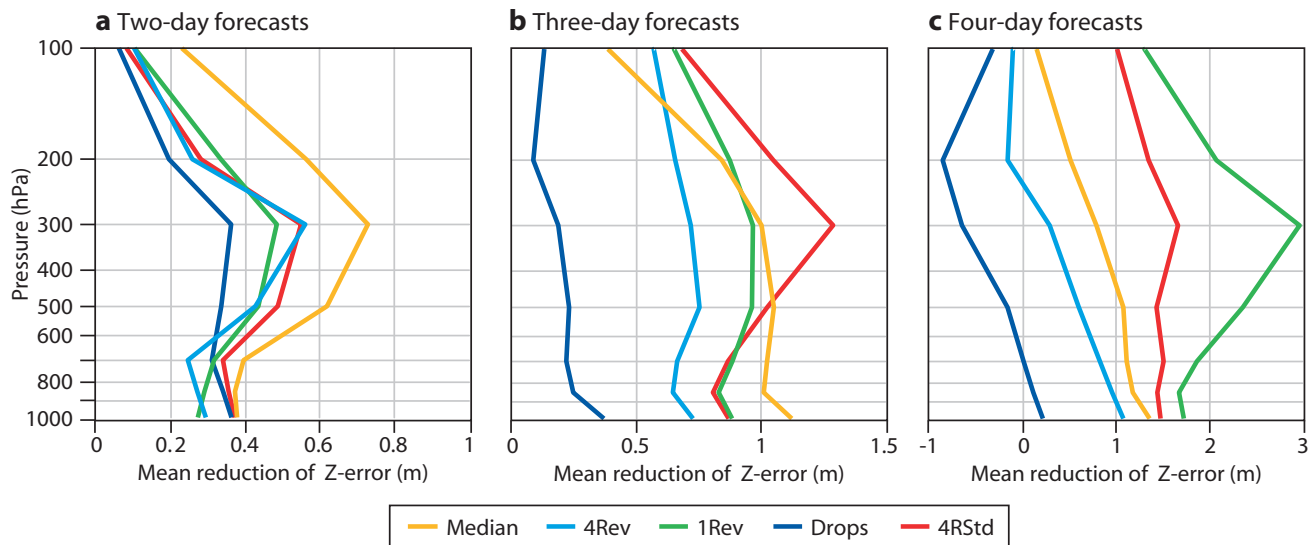


Figure 6 Vertical profile of the mean reduction of the errors of the geopotential height over Europe for (a) two-day forecasts, (b) three-day forecasts and (c) four-day forecasts. The mean reduction was calculated in the same way as in Figure 5 for all 29 forecasts between 14 and 28 November 2003.

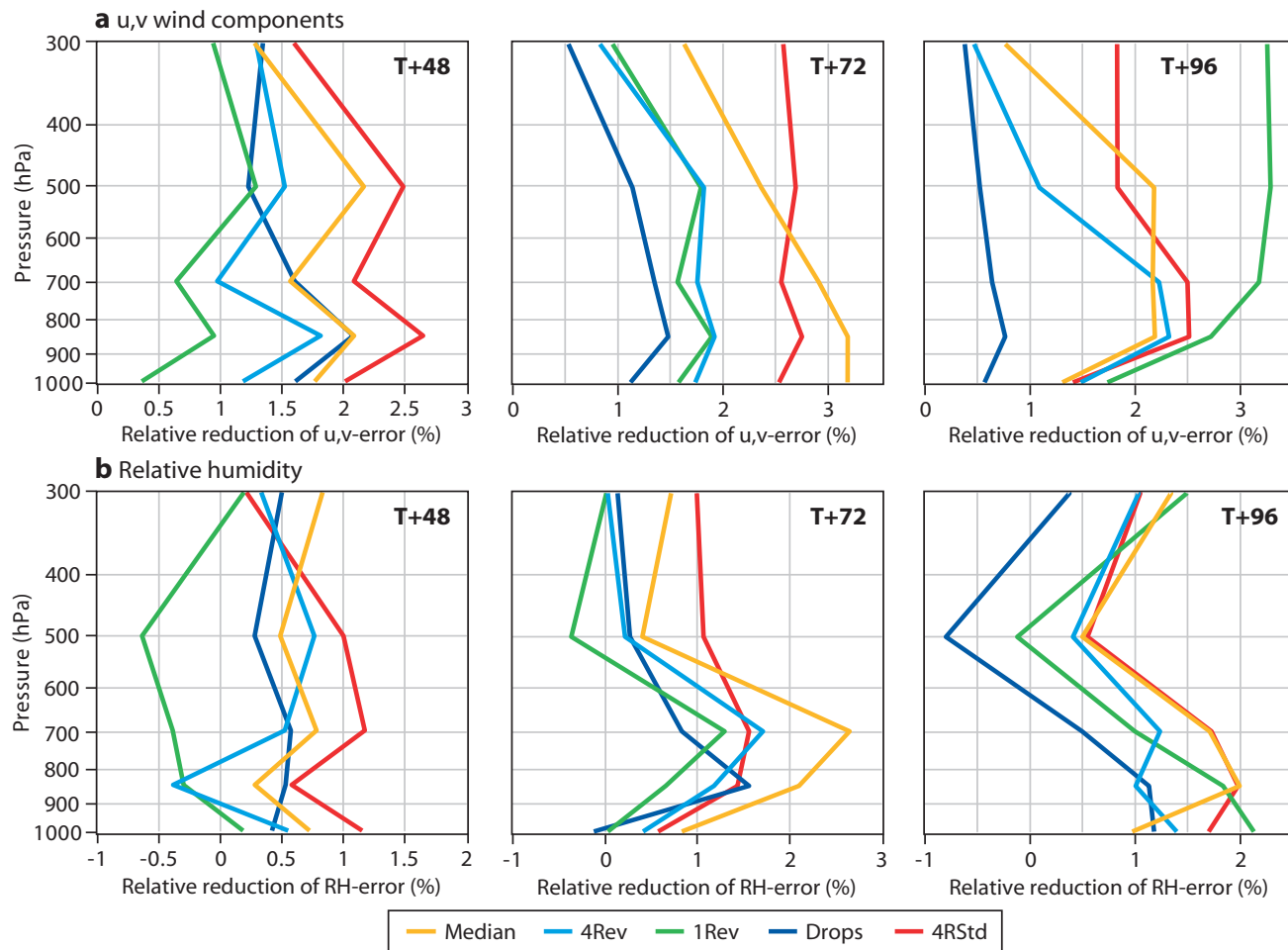


Figure 7 Mean relative reduction of forecast error for (a) u, v wind components and (b) relative humidity over Europe: (left) two-day forecasts, (middle) three-day forecasts and (right) four-day forecasts. All values are in percent of the mean forecast error in the period of 14 to 28 November 2003. The relative reduction was calculated in the same way as in Figure 5, but for humidity and the wind components instead of geopotential height.

The experiment assimilating vertical profiles of wind and temperature from dropsondes for the same period shows only a mean reduction of ~1%, which is consistent with the smaller analysis impact of these observations compared to lidar data. Keeping in mind that the cost of lidar observations is comparable to the cost of dropsondes for the same flight time, the results given here show the potential of the airborne Doppler lidar for future observational campaigns.

Future outlook

Our results underline the importance of additional wind measurements over the oceans and demonstrate the potential of Doppler lidars. These findings support the high expectations for the satellite-based Doppler lidar ADM-Aeolus, which is planned to be launched in 2008 by the European Space Agency (ESA) (Stoffelen et al., 2005). ADM-Aeolus will provide a global coverage (3,000 profiles of LOS velocity per day), but the accuracy of ADM-Aeolus will only be half that of the airborne lidar and the vertical resolution is 500–1,000 m instead of 100 m. Given these differences, mounting Doppler lidars on commercial aircraft to provide wind profiles

over oceans with high accuracy and high resolution should be investigated.

Specific investigations of the impact of lidar data in the verification regions established by the targeting techniques will be carried out in subsequent studies. Furthermore, sensitivity studies are planned that investigate the impact of data accuracy, horizontal and vertical resolution, and data thinning. Experiments on the impact of differential absorption lidar (DIAL) water vapour measurements from different campaigns started recently in collaboration between DLR and ECMWF.

In the summer of 2007 the wind and the water vapour lidar system of DLR operated simultaneously on one aircraft for the first time. This configuration will be deployed during several field campaigns and is expected to provide a large dataset of collocated wind and water vapour observations for investigating the potential of lidars for the future observing system. In the near future research activities with airborne lidars will primarily focus on the THORPEX Pacific Asian Regional Campaign (T-PARC) in the second half of 2008, but a European THORPEX campaign is coming up in the time-frame of 2010/2011.

FURTHER READING

Cardinali, C., S. Pezzulli & E. Andersson, 2004: Influencematrix diagnostic of a data assimilation system. *Q.J.R. Meteorol. Soc.*, **130**, 2767–2786.

Cress, A. & W. Wergen, 2001: Impact of profile observations on the German Weather Service's NWP system. *Meteorol. Zeitschrift*, **10**, 91–101.

Stoffelen, A., J., Pailleux, E. Källén, J.M. Vaughan, L. Isaksen, P. Flamant, W. Wergen, E. Andersson, H. Schyberg, A. Culoma, R. Meynart, M. Endemann, M. &

P. Ingmann, 2005: The Atmospheric Dynamics Mission for global wind field measurement. *Bull. Am. Meteorol. Soc.*, **86**, 73–87.

Weissmann, M., R. Busen, A. Dörnbrack, S. Rahm & O. Reitebuch, 2005: Targeted observations with an airborne wind lidar. *J. Atmos. Ocean. Technol.*, **22**, 1706–1719.

Weissmann, M. & C. Cardinali, 2007: The impact of airborne Doppler lidar measurements on ECMWF forecasts. *Q.J.R. Meteorol. Soc.*, **133**, 107–116.